

Phase behavior of rotationally asymmetric Brownian kites containing 90° internal angles

Huaqing Liu(柳华清), Yiwu Zong(宗奕吾), Zhanglin Hou(侯章林), Thomas G. Mason, and Kun Zhao(赵坤)
Citation: Chin. Phys. B, 2021, 30 (**12**): 124701. DOI: 10.1088/1674-1056/ac306c
Journal homepage: http://cpb.iphy.ac.cn; http://iopscience.iop.org/cpb

What follows is a list of articles you may be interested in

Non-Stokes drag coefficient in single-particle electrophoresis:New insights on a classical problem

Mai-Jia Liao(廖麦嘉), Ming-Tzo Wei(魏名佐), Shi-Xin Xu(徐士鑫), H Daniel Ou-Yang(歐陽新喬), Ping Sheng(沈平)
Chin. Phys. B, 2019, 28 (**8**): 084701. DOI: 10.1088/1674-1056/28/8/084701

Dramatic change of the self-diffusions of colloidal ellipsoids by hydrodynamic interactions in narrow channels

Han-Hai Li(李瀚海), Zhong-Yu Zheng(郑中玉), Tian Xie(谢天), Yu-Ren Wang(王育人)
Chin. Phys. B, 2019, 28 (**7**): 074701. DOI: 10.1088/1674-1056/28/7/074701

Relationship between characteristic lengths and effective Saffman length in colloidal monolayers near a water-oil interface

Na Li(李娜), Wei Zhang(张伟), Wei Chen(陈唯)
Chin. Phys. B, 2019, 28 (**6**): 064703. DOI: 10.1088/1674-1056/28/6/064703

Coupling effect of Brownian motion and laminar shear flow on colloid coagulation:a Brownian dynamics simulation study

Xu Sheng-Hua,Sun Zhi-Wei,Li Xu,Tong Wang
Chin. Phys. B, 2012, 21 (**5**): 054702. DOI: 10.1088/1674-1056/21/5/054702

Phase behavior of rotationally asymmetric Brownian kites containing 90° internal angles*

Huaqing Liu(柳华清)[1,†], Yiwu Zong(宗奕吾)[1,†], Zhanglin Hou(侯章林)[2], Thomas G. Mason[3,4,‡], and Kun Zhao(赵坤)[1,5,§]

[1] *Key Laboratory of Systems Bioengineering (Ministry of Education), School of Chemical Engineering and Technology, Tianjin University, Tianjin* 300072, *China*

[2] *Wenzhou Institute, University of Chinese Academy of Sciences, Wenzhou* 325001, *China*

[3] *Department of Physics and Astronomy, University of California-Los Angeles, Los Angeles, CA* 90095, *USA*

[4] *Department of Chemistry and Biochemistry, University of California-Los Angeles, Los Angeles, CA* 90095, *USA*

[5] *Physics Department, Tianjin University, Tianjin* 300072, *China*

(Received 11 September 2021; revised manuscript received 8 October 2021; accepted manuscript online 18 October 2021)

Previous Monte Carlo simulations have shown that ordered tetratic phases can emerge in a dense two-dimensional Brownian system of rotationally asymmetric hard kites having 90° internal angles. However, there have been no experimental investigations yet to compare with these simulation results. Here, we have fabricated two types of micron-sized kites having internal angles of 72°–90°–108°–90° and 72°–99°–90°–99°, respectively, and we have experimentally studied their phase behavior in two-dimensional systems. Interestingly and in contrast to the Monte Carlo simulations, the experimental results show a phase sequence of isotropic fluid-hexagonal rotator crystal-square crystal as the area fraction ϕ_A increases for both types of kites. The observed square crystal displays not only a quasi-long-range translational order but also (quasi-)long-range 4-fold bond- and molecular-orientational order; these characteristics confirm that tetratic order can emerge even in dense Brownian systems of rotationally asymmetric particles. A model based on local polymorphic configurations (LPCs) is proposed to understand the origin of the square lattice order in these dense kite systems. The results in this study provide a new route to realize custom-designed self-assembly of colloids by controlling LPCs.

Keywords: tetratic order, colloidal kites, two-dimentional system, phase behavior

PACS: 47.57.J–, 03.65.Vf, 75.40.Cx **DOI:** 10.1088/1674-1056/ac306c

1. Introduction

Colloids, due to their relatively large size and easily tunable properties, have long been used as models for atomic and molecular systems for studying fundamental questions in condensed matter physics, such as crystallization, glassy states, and the glass transition.[1–10] The hard sphere model is one of such model system that has been studied extensively and its phase behavior is understood very well.[11–14] As the particle volume fraction increases, a three-dimensional (3D) hard sphere system shows a disorder-order transition from an isotropic fluid phase to a face-centered cubic crystalline phase.[11,12,15] Compared with simple spherical colloids, anisometric colloids, like ellipsoids,[16–19] and rods,[20,21] have discernable orientations and thus can show a variety of phases that are not accessible for hard spheres, such as nematic, smectic, or tetratic liquid crystals. Particularly, with the advances in the fabrication techniques of anisotropic colloids, the pool of available anisometric-shaped colloids are continuously expanding, and additional interesting new phases have been observed.[22] Despite such progress, our understanding of the relationship between the shape of colloids and their phase behavior is still far from complete. One possible reason is due to the enormous range of shapes that colloids can have, it is thus difficult to provide a general framework that can be established to predict the forms of self-ordering in slowly crowded Brownian systems of hard anisotropic particles having arbitrary shape. In addition, a recent Monte Carlo simulation study[23] has demonstrated that a single right internal angle in a kite shape, which is rotationally asymmetric, is enough to induce a tetratic order, which has four-fold rotational symmetry, in a slowly crowded Brownian system composed of many such kites. These results pose further difficult questions about how to directly link the symmetry of ordered phases with the symmetry of particle shapes and call for more attention to the role of local polymorphic configurations of complex colloids in understanding phase behavior. However, so far, there has been no experimental investigation to compare with the simulation results of such kites containing right internal angles. Moreover, only expansions were performed in these prior Monte Carlo simulations,[23] so, whether or not the tetratic order can be ob-

*Project supported by the National Natural Science Foundation of China (Grant Nos. 11874277 and 21621004, and 11704276) and the Natural Science Foundation of Tianjin, China (Grant No. 19JCQNJC14900).

†These authors contributed equally to this work.

‡Corresponding author. E-mail: mason@chem.ucla.edu

§Corresponding author. E-mail: kunzhao@tju.edu.cn

© 2021 Chinese Physical Society and IOP Publishing Ltd

served under slow compression in a thermal Brownian system is still not clear.

To address these questions, we investigate the phase behavior of two-dimensional Brownian kite systems for two differently shaped kites: one has internal angles of 72°–90°–108°–90° (herein called the 108°-kite), and the other has 72°–99°–90°–99° (herein called the 90°-kite). By optically measuring, analyzing, and characterizing different phases using order parameters and correlation functions, phase diagrams of these two kite systems were obtained. A model based on local polymorphic configurations (LPCs) was also proposed to understand the crystalline nature of these systems.

2. Experimental methods

We prepared two kinds of kite-platelets, composed of crosslinked SU-8 polymer, by high-fidelity stepper photolithography.[24] The corners of the kites are slightly rounded with an average radius of curvature 0.30 ± 0.05 μm since the stepper's minimum feature size ($\sim$ 300 nm) is limited. After mixing the kite-platelets with sodium dodecyl sulfate (SDS, stabilizer, final concentration after mixing is $\sim$ 1 mM, purchased from Energy Chemical, GR) and polystyrene (PS) spheres (depletion agent with a diameter of 20 nm, final concentration after mixing is $\sim$ 1.0% w/v, purchased from ThermoFisher), we filled the aqueous dispersion of particles into a rectangular glass tube (VitroCom), which was then sealed using photosensitive adhesive (Norland NOA81). The whole glass tube was then fixed to a glass slide using adhesive.

3. Results and discussion

The two types of four-sided colloidal kite platelets were mass produced photo-lithographically (see Section 2). Each 108°-kite has two long edges of 2.9 ± 0.9 μm, two short edges of 2.1 ± 0.7 μm, and a thickness of 1.6 ± 0.1 μm (see Fig. 1(a) inset for a microscopic image taken using scanning electron microscopy), while each 90°-kite has two long edges of 3.1 ± 0.8 μm, two short edges of 2.6 ± 0.6 μm, and a thickness of 1.7 ± 0.1 μm (Fig. S3(a) inset). Kites of each type were dispersed in an aqueous SDS solution in a rectangular tube together with 1%w/v 20-nm diameter polystyrene, which serve as a depletion agent. Roughness-controlled depletion attractions[24,25] cause the platelets to be attracted to the bottom surface of glass tube to form a monolayer in which the kite colloids behave like hard-particles and freely diffuse. To compress the two-dimensional monolayer in a near-equilibrium manner, the tube was slightly titled along its long axis by $\sim 3.5°$ over a duration of about 3 months for equilibration; this process yielded a slowly varying spatial gradient in area fraction ϕ_A. Then, images were taken at various locations along the tube for assembled structures with different ϕ_A (*i.e.*, degree of osmotic compression) with an inverted optical microscope (Leica DMi8) using a long working distance 63X objective (numerical aperture 0.7). Each image has a size of 52.1 μm $\times$ 52.1 μm, and can contain up to $\sim$ 300 108°-kites (or $\sim$ 250 90°-kites) at high ϕ_A. Although a larger field of view can contain more particles, it is not suitable for image analysis due to the possible non-negligible density gradient effect and additional defects included. These images were then digitally processed to extract centers and vertices of kites for further analysis using user-written Interactive Data Language routines (see Fig. S1 for examples).

The experimentally observed phase behavior of 108°-kite and 90°-kite is similar. So in the main text, we mainly present results of 108°-kite. Figure 1 shows the phase sequence of the 108°-kite system as ϕ_A increases. At a relatively low $\phi_A = 0.48$, no obvious order is observed in the optical micrograph and its corresponding Fourier transforms (FT) shows a typical ring pattern (Fig. 1(a)), which is a characteristic of isotropic fluid phase (I). As ϕ_A increases to 0.54, 6-fold translational order develops in the system, as evidenced by its FT pattern which displays six sharp bright spots separated by $\sim 60°$. But the orientation of colloids is still random, so the system at $\phi_A = 0.54$ is in a hexagonal rotator crystal (RX) phase. Surprisingly, at higher $\phi_A = 0.68$, a square phase (SQ) is observed in which kites are positioned approximately on a square lattice and their orientations display a tetratic order (*i.e.*, has a four-fold rotational symmetry, which will be quantitatively characterized later). The FT of the corresponding optical micrograph shows four sharp bright spots separated by 90° and confirms the square lattice. Between RX and SQ phases, there is a co-existence region of both hexagonal and square domains observed (see domain examples shown in Fig. 1(c)).

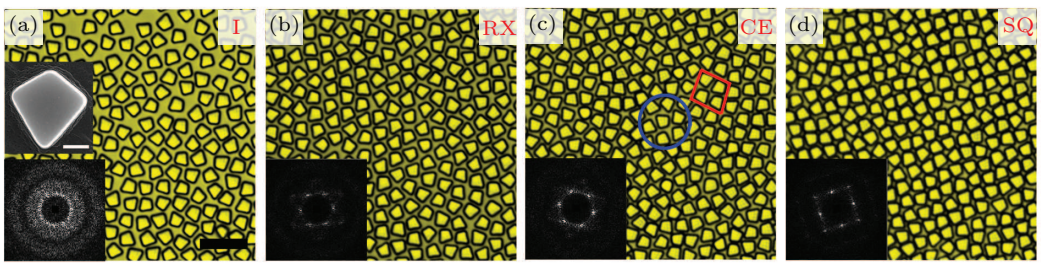


Fig. 1. Optical micrographs of 108°-kites at various area fractions ϕ_A: (a) $\phi_A = 0.48$, isotropic fluid phase (I), (b) $\phi_A = 0.54$, rotator hexagonal crystal phase (RX), (c) $\phi_A = 0.61$, coexistence (CE), and (d) $\phi_A = 0.68$, square phase (SQ). Inset, upper left conner of panel (a): SEM image of a 108°-kite, scale bar is 1 μm. Insets, lower left corners: Fourier transforms of corresponding micrographs. Scale bar,10 μm.

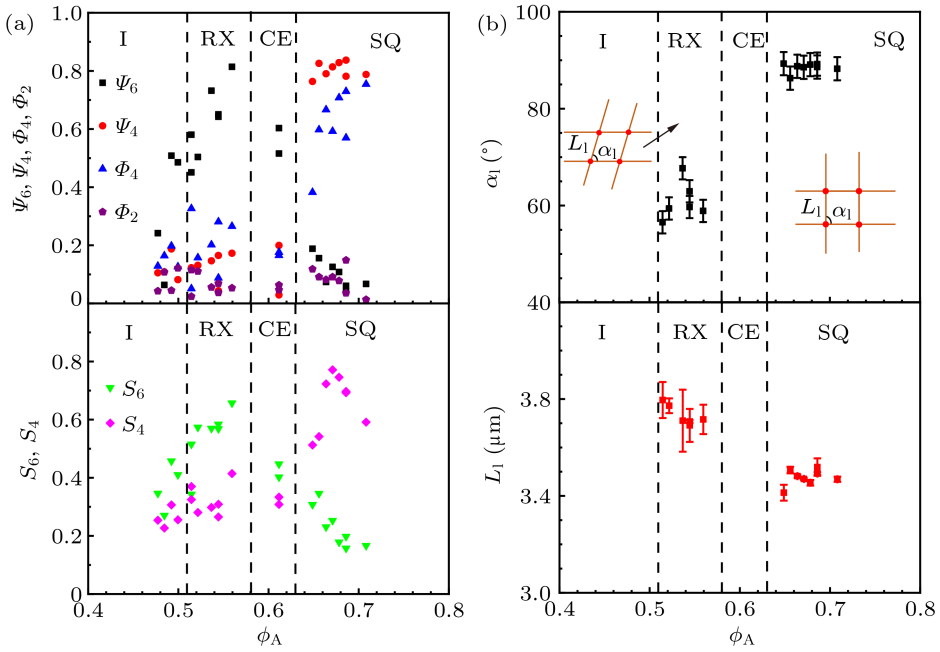


Fig. 2. (a) Measured spatial and orientational order parameters as a function of ϕ_A, including global 6-fold spatial (S_6, green downward triangle) and bond-orientational (Ψ_6, black square) order parameters, 4-fold spatial (S_4, magenta diamond), bond-orientational (Ψ_4, red circles), and molecular-orientational (Φ_4, blue upward triangle) order parameters and 2-fold molecular-orientational (Φ_2, purple pentagon) order parameter; (b) the lattice angle α_l and center-to-center spacing L_l of crystalline phases as a function of ϕ_A.

Quantitatively, different phases are characterized by order parameters and correlation functions, including global 6-fold spatial (S_6) and bond-orientational (Ψ_6) order parameters, 4-fold spatial (S_4), bond-orientational (Ψ_4), and molecular-orientational (Φ_4) order parameters, 2-fold molecular-orientational (Φ_2) order parameter as well as their corresponding correlation functions (see supplementary information for more details). Figure 2(a) shows the results of order parameters. We can see that when ϕ_A is low (< 0.51) and the system is in I phase, the 4-fold order parameters S_4, Ψ_4, and Φ_4 are kept small while the 6-fold order parameters S_6 and Ψ_6 are also relatively low but rise as ϕ_A increases. When ϕ_A increases above 0.51 but below 0.58, S_6 and Ψ_6 reach to a high value (≥ 0.5) while Ψ_4 and Φ_4 increase slightly and stay low. So, for this range of ϕ_A we classify the system to be in an RX phase. The lattice angle of RX phase α_l is $\sim 60^\circ$ and the lattice spacing L_l is reduced from 3.8 μm to 3.7 μm with ϕ_A increases (Fig. 2(b)). As ϕ_A continues to increase above 0.58, 6-fold and 4-fold order parameters show a quick but opposite change with Ψ_6 and S_6 going down while Ψ_4, S_4, and Φ_4 going up. Then, when $\phi_A \geq 0.63$, Ψ_4 and S_4 all reach a high value (≥ 0.6) indicating the system is in an SQ phase. In this phase, α_l is $\sim 90^\circ$ and L_l in general follows a trend to decrease from 3.5 μm to 3.4 μm with ϕ_A increases. Moreover, in the SQ phase, Φ_4 is high (≥ 0.6) while Φ_2 is still low as in other phases, indicating that in the SQ phase, although the centers of mass of kites are positioned on a square lattice, particles are not uniformly pointed but rather can point along two perpendicular directions, *i.e.*, the SQ phase has tetratic order in molecular orientations. The surface fraction then exhibits a jump from RX to SQ phase; this feature together with the sharp change in the 4-fold order parameters and the previously observed coexistence region of hexagonal and square domains, supports the first-order transition of RX-SQ.

Figure 3 shows the results of correlation functions, which can characterize the extent of range to which specific order can correlate for different phases observed in Fig. 1. For example, within the tested range of r/L, in I phase, both translational and orientational correlation functions decay quickly to a background level (Figs. 3(a)–3(e)), indicating short-range orders of the system; while in RX phase, 4-fold bond-orientational g_4^{bo}, spatial g_{sq}, and molecular-orientational g_4^{mo} correlation functions decay quickly to a background level, whereas 6-fold bond-orientational correlation function g_6^{bo} first decays from 0.6 to 0.4 and then keeps at 0.4, and 6-fold spatial correlation function g_{hex} also decays more slowly than an algebraic decay with an exponent of $-1/3$, indicating a quasi-long-range 6-fold bond-orientational and translational order of the system. By contrast, in SQ phase, all 6-fold correlation functions decay quickly to a background level, whereas both g_4^{bo} and g_4^{mo} display a plateau with a high value (≥ 0.5) at large r/L, indicating a (quasi-)long-range tetratic order in both bond- and molecular-orientations. Please note that due to the limited size of available uniform single crystal regions in our systems, we do not have enough spatial range to unambiguously conclude the long-range tetratic order observed in SQ phase. g_{sq} also decays more slowly than an algebraic decay with an exponent of $-1/3$, suggesting a quasi-long-range

translational order of the system. In addition, pair correlation functions $g(r/L)$ are also calculated (Fig. 3(f)) (L is the length of the long diagonal of 108°-kite). As we expect, compared with disordered I phase, RX and SQ phases show relatively sharp peaks in $g(r/L)$, consistent with their stronger translational order. But the peaks of $g(r/L)$ in RX phase deviate from those obtained from an ideal hexagonal lattice possibly due to the shift of the mass center of kites from perfect lattice sites resulted from random orientations of these rotationally asymmetric kites. By contrast, the peaks of $g(r/L)$ in SQ phase match reasonably well with those obtained from an ideal square lattice. This is also consistent with the observation that $g_{\rm sq}$ approaches to a higher plateau value than $g_{\rm hex}$ at large r/L.

To understand the origin of SQ phase appeared in dense systems of 108°-kite, we listed all the local polymorphic configurations (LPCs) of 108°-kite, each of which is formed by 3–5 particles with the constrain that the vertices of the component kites should meet at a central point and the sum of internal angles around the point should be within (288°, 360°] so that there is no more kite that can be added into the configuration. This method is similar to the one used in Ref. [26]. The results are shown in Fig. 4(a). For LPCs consisting of three kites or five kites, there are three or one kind(s) of configuration, respectively, while for LPCs consisting of four kites, there are 32 kinds of configuration. Supposing all configurations have equal probability to form, apparently 4-kite LPCs will dominate. Each 4-kite LPC corresponds to a quadrilateral formed by the mass centers of four kites. By calculating the four internal angles (denoted by γ) and the lengths (denoted by l) of the four edges of each quadrilateral (for the cases of LPC whose sum of internal angles at the meeting point is less than 360°, we choose a simple configuration, in which the four kites are rotationally equally separated, as an example to obtain the quadrilateral and its associated internal angles and edge lengths), we performed a histogram analysis (Fig. 4(b)) and found that a majority of γ are within [85°, 95°], and most of l are within a narrow range of [2.3 μm, 2.7 μm]. Such closely related shapes of quadrilateral also make 4-kite LPCs compatible with each other in terms of structural symmetry. Taken together, these results indicate that because 4-kite LPCs have the largest probability to appear among all LPCs and they are more or less compatible due to similar quadrilateral shapes, the system can develop a global (within the tested range) square lattice ($\alpha_{\rm l} \sim 90°$) with 4-kite LPCs as unit building blocks. This is also supported by a tessellation result of an optical micrograph at $\phi_{\rm A} = 0.68$ (in SQ phase) using these 4-kite LPCs (Fig. S2), which shows that a majority of kites can be covered by such 4-kite LPCs. We would like to point out that the current LPCs model only considers the packing of kites within each different type of LPC. However, to fully understand the self-assembled global structures, an extended and more complicated model that includes the interactions between these different LPCs such as the compatibility of edges of two neighboring LPCs is needed, which will be a subject of future work.

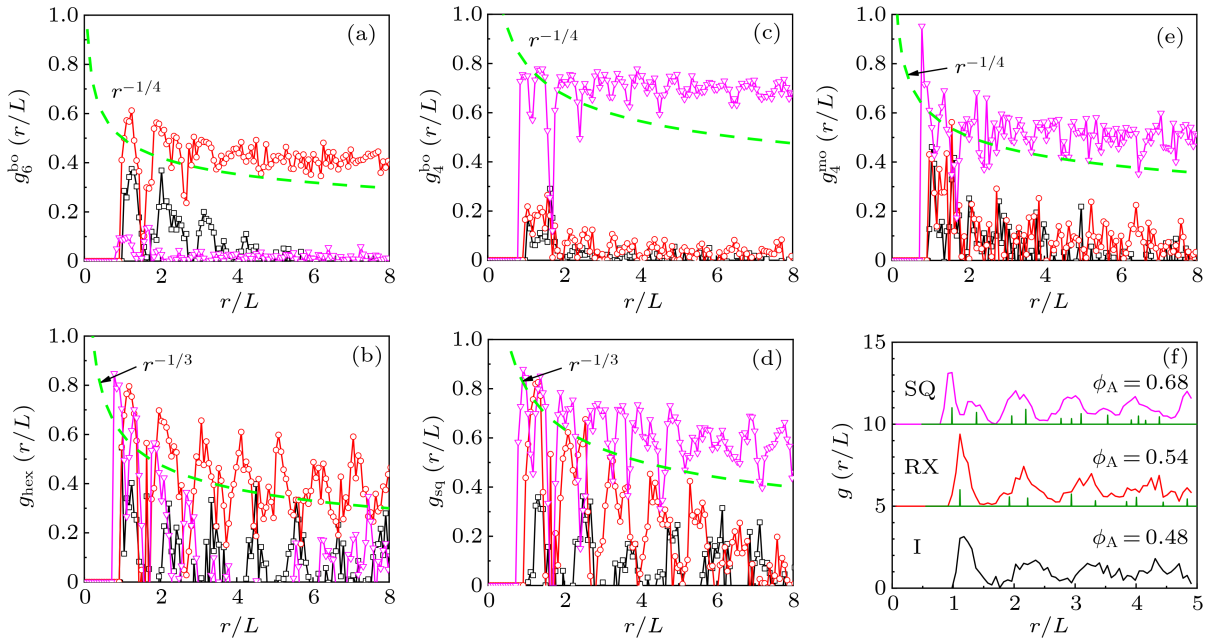


Fig. 3. Correlation functions calculated for different phases of 108°-kite: (a) 6-fold bond-orientational correlation functions $g_6^{\rm bo}(r/L)$; (b) spatial correlation functions related to hexagonal order $g_{\rm hex}(r/L)$; (c) 4-fold bond-orientational correlation functions $g_4^{\rm bo}(r/L)$; (d) spatial correlation functions related to square order $g_{\rm sq}(r/L)$; (e) 4-fold molecular-correlation functions $g_4^{\rm mo}(r/L)$; and (f) spatial pair correlation functions $g(r/L)$, calculated from images in Fig. 1. Black squares, $\phi_{\rm A} = 0.48$ in I phase; red circles, $\phi_{\rm A} = 0.54$ in RX phase; magenta downward triangles, $\phi_{\rm A} = 0.68$ in SQ phase. In panel (f), green delta spikes at $\phi_{\rm A} = 0.68$ and $\phi_{\rm A} = 0.54$ indicate peaks of $g(r/L)$ for perfect hexagonal and square lattices. The dashed line $r^{-1/4}$, is the KTHNY prediction for orientational correlation functions at the liquid crystal-isotropic phase transition point. The dashed line $r^{-1/3}$, is the KTHNY prediction for spatial correlation functions at the crystal–liquid crystal transition point.

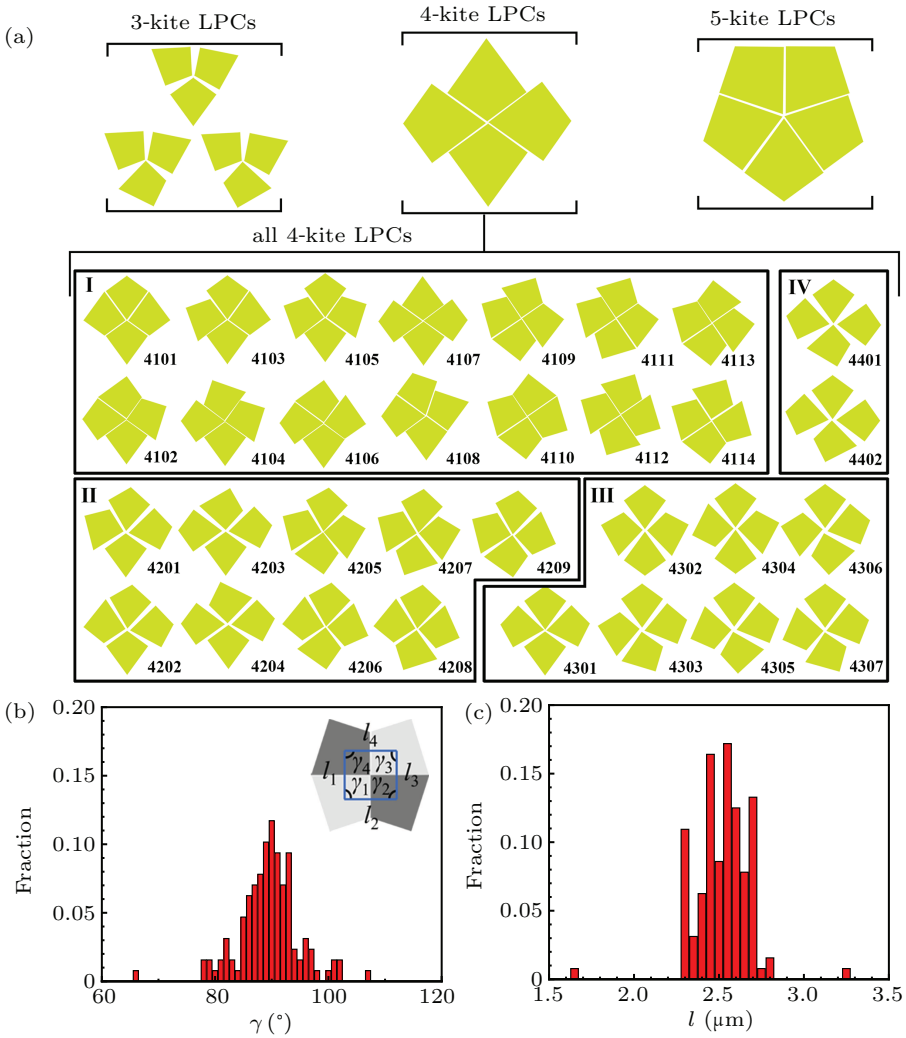


Fig. 4. (a) Schematic illustration showing all LPCs that 108°-kites can form with the constrain that the vertices of the component kites should meet at a central point and the sum of internal angles around the point should be within (360°–72°, 360°]. The 4-kite LPCs are grouped based on the deviation of the sum of internal angles from 360°. Groups I–IV correspond to a deviation of 0°, −18°, −36° , and −54° , respectively; The distribution of (b) internal angles γ and (c) the edge lengths l of all quadrilaterals formed by 4-kite LPCs.

Previous Monte Carlo simulations have shown that 108°-kites can form tetratic ordered phases including tetratic liquid crystal and tetragonal rectangular crystal (TRX).[23] The experimental observations in this study confirm that 108°-kites can form tetratic ordered phases as the SQ phase has four-fold rotational symmetry in both bond- and molecular-orientations. However, neither tetratic liquid crystal nor TRX phase has been observed experimentally. On the other hand, the RX phase and SQ phase are neither observed in Monte Carlo simulations. One of possible reasons leading to such discrepancies would be the different processes employed to study the phase behavior of kites. In MC simulations, an expansion process was employed which started from an ordered alternating striped crystal (ASX) structure. By contrast, in this experimental study, the phase diagram was obtained by slowly compressing the kite system in a near-equilibrium manner. The different dynamic evolution of particles between expansion and compression can lead to different phase behaviors, which has also been observed in other systems.[23,26,27] For example, although regular pentagons can form ASX,[27] experimental results show that they are trapped in a glassy state when they are compressed toward high densities even under a slow, near-equilibrium compression manner.[26] Another possible reason would be the corner-rounding effect[24] of 108°-kites used in experiments which deviate from the mathematically ideal shape used in MC simulations.

In order to better understand the role of 90° internal angle of kites in their self-assembled structures, the phase behavior of 90°-kites which has 72°–99°–90°–99° internal angles is also investigated (Figs. S3–S5 in supplementary information). The results show a phase sequence of I–RX–SQ as ϕ_A increases, same as that for 108°-kites. However, there are differences in the phase behavior between these two shapes. Firstly, RX phase appears at higher ϕ_A in 90°-kites than in 108°-kites. This may be due to the geometry factor that the shape of 108°-kite having an aspect ratio of 1.05 is less anisotropic than the shape of 90°-kite having an aspect ratio of 1.19.[23] Secondly, compared with the case of 108°-kite where SQ phase can be observed in a ϕ_A range of 0.63 ∼ 0.72, in 90°-kites SQ phase is observed only at $\phi_A \sim 0.75$, indicating that it may not easy

for 90°-kites to form square lattice. As a 108°-kite has two 90° internal angles while a 90°-kite has only one, we may guess the more number of 90° internal angles of a kite, the easier for them to form square lattice. However, square colloids that have four 90° internal angles were observed experimentally to form rhombic crystal lattice instead of square lattice at high ϕ_A.[24] Moreover, simulation results in Ref. [23] show that the tetratic order can also form in kites without 90° internal angles. Based on these considerations, we can not draw a conclusion on the direct correspondence between the number of 90° internal angles and the difficulty in forming square lattice. Rather, based on this study and earlier reports,[23,26] we suggest that the local polymorphic configurations (which of course are closely related to particle shape) play an even more important role than pure particle's geometric shape in determining the self-assembled structures when the system is under slowly compressed, and thus should be paid more attention in future work whenever there is a need to fabricate new functional materials through self-assembly of custom-shaped colloids.

4. Conclusion

In this study, the phase behavior of two-dimensional colloidal systems composed of rotationally asymmetric kites having internal angles of 72°–90°–108°–90° and alternatively of 72°–99°–90°–99° have been investigated. For both types of kites, a phase sequence of I-RX-SQ is observed as ϕ_A increases. Although this experimentally obtained phase sequence is different from the one obtained by MC simulations, it nevertheless confirms that tetratic order which has four-fold rotational symmetry, can emerge in dense systems of slowly crowded Brownian particles with no rotational symmetries. Moreover, by contrast to the discrete plastic crystals in earlier reports that show only short-range order in molecular-orientation,[28] the four-fold molecular orientational order in the observed SQ phase of kites is long-range, at least over the limited spatial extent that our experiments permits. Although surprising, this observed discrete SQ phase can be understood by employing an LPC model, which shows that among all LPCs, 4-kite LPCs are dominant and their corresponding quadrilaterals have internal angles around 90° and similar edge lengths. All of these properties facilitate the formation of square lattice by using 4-kite LPCs as unit building blocks for the next larger spatial scale in the hierarchy beyond the particle scale. Although 90°-kites and 108°-kites show a similar phase sequence, they also show differences for example in the phase boundaries of RX and SQ phases. This may be due to the difference in the number of 90° internal angles. However, to test this hypothesis, more work is needed. Moreover, the results in this study show the importance of local polymorphic configurations in determining the final assembled structures and thus, the specific study herein points to a new route to realize custom-designed self-assembly of colloids by controlling LPCs beyond the single-particle scale.

References

[1] Russel W B, Saville D A and Schowalter W R 1992 *Colloidal dispersions*, Vol. 54 (Cambridge, UK: John Wiley & Sons, Ltd)
[2] Gasser U, Weeks E R, Schofield A, Pusey P N and Weitz D A 2001 *Science* **292** 258
[3] Anderson V J and Lekkerkerker H N W 2002 *Nature* **416** 811
[4] Poon W 2004 *Science* **304** 830
[5] Alsayed A M, Islam M F, Zhang J, Collings P J and Yodh A G 2005 *Science* **309** 1207
[6] Mattsson J, Wyss H M, Fernandez-Nieves A, Miyazaki K, Hu Z, Reichman D R and Weitz D A 2009 *Nature* **462** 83
[7] Wang Z, Wang F, Peng Y, Zheng Z and Han Y 2012 *Science* **338** 87
[8] Manoharan V N 2015 *Science* **349** 1253751
[9] Anderson J A, Antonaglia J, Millan J A, Engel M and Glotzer S C 2017 *Phys. Rev. X* **7** 021001
[10] Ma X, Mishra C K, Habdas P and Yodh A G 2021 *J. Chem. Phys.* **155** 074902
[11] Pusey P N and van Megen W 1986 *Nature* **320** 340
[12] Zhu J, Li M, Rogers R, Meyer W, Ottewill R H, Russel W B, Chaikin P M and Crew S T S S S 1997 *Nature* **387** 883
[13] Kegel W K and Blaaderen A V 2000 *Science* **287** 290
[14] Weeks E R, Crocker J C, Levitt A C, Schofield A and Weitz D A 2000 *Science* **287** 627
[15] Cheng Z, Chaikin P M, Russel W B, Meyer W V, Zhu J, Rogers R B and Ottewill R H 2001 *Materials & Design* **22** 529
[16] Vieillard-Baron J 1972 *J. Chem. Phys.* **56** 4729
[17] Yunker P J, Chen K, Zhang Z, Ellenbroek W G, Liu A J and Yodh A G 2011 *Phys. Rev. E* **83** 011403
[18] Zheng Z, Ni R, Wang F, Dijkstra M, Wang Y, Han Y 2014 *Nat. Commun.* **5** 3829
[19] Mizani S, Gurin P, Aliabadi R, Salehi H and Varga S 2020 *J. Chem. Phys.* **153** 034501
[20] Bates M A and Frenkel D 2000 *J. Chem. Phys.* **112** 10034
[21] Donev A, Burton J, Stillinger F H and Torquato S 2006 *Phys. Rev. B* **73** 054109
[22] Glotzer S C and Solomon M J 2007 *Nat. Mater.* **6** 557
[23] Hou Z, Zong Y, Sun Z, Ye F, Mason T G and Zhao K 2020 *Nat. Commun.* **11** 2064
[24] Zhao K, Bruinsma R and Mason T G 2011 *Proc. Natl. Acad. Sci. USA* **108** 2684
[25] Zhao K and Mason T G 2007 *Phys. Rev. Lett.* **99** 268301
[26] Zhao K and Mason T G 2015 *Proc. Natl. Acad. Sci. USA* **112** 12063
[27] Schilling T, Pronk S, Mulder B and Frenkel D 2005 *Phys. Rev. E* **71** 036138
[28] Shen W, Antonaglia J, Anderson J A, Engel M, van Anders G and Glotzer S C 2019 *Soft Matter* **15** 2571